A METHOD TO PREDICT THE THERMAL CONDUCTANCE OF A BOLTED JOINT

John E. Fontenot, Jr.* and Charles A. Whitehurst**

Abstract

A practical analytical method was developed to predict the interface thermal conductance of a bolted joint from a minimum of design information. Simple equations were developed to describe the thermal conductance across the interfacial contact zone and the interfacial gap. Use was made of methods, described in a previous paper, to determine the interfacial contact pressures and the width of the interface gap. Calculated values of interface conductance were used in finite-difference heat transfer analyses and the computed interface temperatures compared to values measured in nine experiments.

Nomenclature

$\bar{a}$	Average radius of contact points (spots)
C_a	Thermal conductance of contact points
C_D	Thermal conductance due to conduction across interface fluid
C_f	Thermal conductance of interface fluid
C_g	Thermal conductance across interface gap
C_R	Thermal conductance due to radiation across interface gap
C_t	Total conductance of joint contact area
H	Meyer hardness
H_o	Nominal Meyer hardness
i_A	R.M.S. of surface irregularity - surface A
i_B	R.M.S. of surface irregularity - surface B
k	Thermal conductivity
k_f	Thermal conductivity of interface fluid

*Mechanical Engineer, Shell Development Company, Mechanical Engineering Research Department, Houston, Texas; Member ASME; formerly a graduate student in Mechanical Engineering at Louisiana State University.

**Associate Professor, Louisiana State University, Division of Engineering Research, Baton Rouge, Louisiana; Member ASME.

k_m	Mean value of thermal conductivity for joint members
n	Number of contact points per unit area
P	Pressure
r_e	One-half of average value of distance between contact points
r_h	Radius of bolthead
r_s	Radius of bolt shank
r_σ	Radial extent of interface stress
T_M	Average temperature of joint interface
$\overline{\delta}$	Average interface gap thickness
δ_R	Equivalent interface gap for radiation
ξ	Empirical constant in equation 2
λ_A	Wave length of surface waviness, surface A
λ_B	Wave length of surface waviness, surface B
ρ_A	R.M.S. value of surface roughness, surface A
ρ_B	R.M.S. value of surface roughness; surface B
σ	Stefan-Boltzmann constant
ψ	Empirical constant in equation 2

Background and Introduction

In most of the work that has been done to measure either the heat transfer across or the thermal conductance of a joint interface, many simplifying assumptions have been made. The mechanical fastener has been eliminated and the problem worked as if the two joint members were pressed together by a uniformly distributed load. The simplification is demonstrated by Figure 1.

There are important differences between the heat transfer problems of actual joints and of contacts. In the actual joint, the thickness of the interface (interface gap) is a function of fastener and joint geometry as well as the torque applied to the fastener. The thickness of this gap varies considerably along the interface. In the idealized joint, the applied load is uniform and the interface stress is macroscopically uniform. The

interface stress varies on a microscopic scale because of irregularities on the contact surfaces. Of primary importance in a study of the thermal conductance of contacts is the consideration of the microscopic roughness. A study of the thermal conductance of a mechanical joint involves, in addition, the determination of the width of and stresses in the macroscopic contact zone, and the thickness of the interface gap. These are functions of the stresses induced in the joint members by the fastener.

The problem of determining the thermal gradients across surfaces in contact was of concern as far back as 1913 (1)*. Numerous papers have been written on this subject, and a very comprehensive bibliography of these was compiled by Atkins (2) in 1965. Two other literature surveys were conducted by Minges (3) in 1966 and Fontenot (4) in 1964. Several papers on the subject of the thermal conductance of contacts will be discussed shortly.

The majority of the papers on the subject of interface conductance is devoted to contact conductance, as opposed to joint conductance. The first known publication devoted to actual mechanical joints is that of Jelinek (5) in 1949. Since that time there have been a number of publications, the most comprehensive one being that of Lindh et al (6). Lindh et al's report was an attempt at a comprehensive analysis of the thermal conductance of riveted joints. Some of the shortcomings of their work are discussed at length in references 4 and 7.

A review of the literature on the subject of the thermal conductance of joints leads one to the conclusion that at the present time there is not a satisfactory approach to the over-all problem. Such an approach should provide the designer or analyst, a method of estimating the temperature distribution in a bolted joint from design information. In the past these estimates have almost always been based on experimental data.

*Numbers in parentheses refer to similarly numbered references in bibliography at end of paper.

The primary objective of the work reported here was the development of a practical analytical method of determining the interface thermal conductance of a bolted joint from a minimum of design information. As a part of this effort, simple equations describing the thermal conductance in the contact zone were developed. Nine experiments were conducted to verify the interface temperatures calculated for two joints under vacuum and atmospheric pressure conditions.

Approach to Heat Transfer Across Bolted Joints

A mathematical model of a bolted joint can be formulated that adequately describes the interfacial heat transfer. The partial differential equations for the steady state temperature distribution in the joint members can be written along with the appropriate boundary conditions. Because of the complexity of the interface conductance and the boundary conditions (reference 7) a closed-form solution for the equations is not possible. However, a solution is readily obtained if a finite-difference approach is used. Two of the many finite-difference programs now in wide use are described in references 8 and 9.

In order to utilize a finite-difference solution, the two plates must be divided into nodes; the interface conductance must then be described for each pair of interface nodes. As the first step, both the regions of apparent contact and the pressure in these regions must be determined and the interface gap calculated as a function of position. Methods developed to do this are discussed in a previous paper by the authors (10). After the contact areas and pressures and the interface gap thickness are established, the interface conductance must be determined as a function of node location.

Methods developed to do this in the contact and separated zones will be taken up in the following paragraphs.

Contact Zone Conductance

A review of the literature on the subject of contact thermal conductance leads to the conclusion that there is little practicality in the great majority of theoretical or semi-empirical methods now available. In other words, it is almost impossible for a designer to take this problem into account without an appreciable amount of testing. As an illustration of this point, four approaches outlined in the literature will be briefly discussed here. These are the work of Fenech and Rohsenow (11), Centinkale and Fishenden (12), Laming (13), and Boeschoten and Van der Held (14).

Fenech's and Rohsenow's approach is very rigorous and complex; it agrees well with the experimental data. Unfortunately, this method requires that two recorded surface profiles of each plate in contact be made and analyzed. In lieu of making surface profiles, one would probably find it easier to actually measure the contact conductance. Obviously, this theoretical approach is not practical for the prediction of contact thermal conductance.

The Centinkale-Fishenden and Laming methods, though not so rigorous as that of Fenech and Rohsenow, require less information about the contact surfaces. In some cases, all the required information may be available. Hence, these two approaches merit greater consideration as possible methods for the theoretical prediction of contact conductance. Therefore, these two methods, along with that of Boeschoten and Van der Held, will be discussed in more detail. The approach taken by Boeschoten and Van der Held requires

very little information about the surface properties and is nearly always applicable.

Centinkale and Fishenden made use of Southwell's relaxation method to derive a theoretical expression for the conductance of metal surfaces in contact. The expression which they obtained for the total conductance is

$$C_t = C_f + C_a = \frac{k_f}{\overline{\delta}} + \frac{k_M (P/H_o)^{\frac{1}{2}}}{r_e \tan^{-1}\left\{\left[(H_o/P)\left(1 - \frac{k_f}{C_t \overline{\delta}}\right)\right]^{\frac{1}{2}} - 1\right\}} \qquad (1)$$

where H_o is the nominal value of Meyer hardness of the softer metal, $k_M = \frac{2k_1 k_2}{k_1 + k_2}$, and r_e is one-half the average value of the distance between contact points. Their approximation for r_e was

$$r_e = \psi(\lambda_A + \lambda_B)\left(\frac{P}{H_o}\right)^{-\zeta} \qquad (2)$$

where λ_A and λ_B are the wave lengths of the surface waviness of surfaces A and B, respectively, and ψ and ζ are constants to be determined experimentally.

Centinkale and Fishenden determined ψ and ζ for ground surfaces to be $\psi = 4.8 \times 10^{-3}$ and $\zeta = 5/6$. These values were independent of the plate material and the interstitial fluid. For surfaces finished by other methods than grinding, different values for ψ and ζ may be needed. Centinkale and Fishenden also found experimentally that

$$\overline{\delta} = 0.61(i_A + i_B) \qquad (3)$$

where i_A and i_B are the root-mean-square values of surface irregularity (roughness plus waviness) for surfaces A and B, respectively. They state that no change in $\overline{\delta}$ with pressure was detectable up to 800 psi. Since contact point conductance increasingly predominates over fluid conductance as the

pressure is increased, the effects of any change in $\bar{\delta}$ on the contact conductance would become very small. They thus assumed that $\bar{\delta}$ is constant.

With equations 1 and 2 combined and the values determined for ψ and ξ inserted, C_a can be written as

$$C_a = \frac{2.08 \times 10^{-4} \, k_M P^{\frac{4}{3}}}{(\lambda_A + \lambda_B) H_o^{\frac{4}{3}} \tan^{-1}\left\{\left[\frac{H_o}{P}\left(1 - \frac{C_a}{C_t}\right)\right]^{\frac{1}{2}} - 1\right\}} \quad (4)$$

For equation 1 to be used, i_A, i_B, λ_A, λ_B must be known. Values of i_A and i_B can be approximated from the specified values of surface finish. If the finishing process is grinding, equation 4 can be used to determine C_a. For other finishing processes, this equation will at least provide an approximation.

If values for λ_A and λ_B are known in a particular case, then equation 4 can provide a fair estimate of the conductance due to the contact points. If numerical values are not available (usually the case in design), then this equation is useless. An attempt was made during the present study to determine if a range of possible values for wave length of surface waviness could be fixed when the quality of surface finish and the machining operation are known. Apparently a correlation between waviness and roughness for a given finishing operation has never been made.

Laming (13) approaches the problem of determining C_t in a somewhat simpler manner than that of Centinkale and Fishenden. The expression that he obtained for C_f is identical to equation 1. However, he found $\bar{\delta}$ to be $0.67(i_A + i_B)$. The expression derived by Laming for C_a, somewhat different from that given by equation 4 is

$$C_a = \frac{1.83 \times 10^{-3} \, k_M P^{\frac{3}{4}}}{(\lambda_A \lambda_B)^{\frac{1}{4}} \left[1 - 2.28 \times 10^{-3} (P)^{\frac{3}{4}} (\lambda_A \lambda_B)^{\frac{1}{4}} \left(1 - \frac{C_f}{C_a}\right)^{\frac{1}{2}}\right]} \quad (5)$$

A comparison of this with equation 4 reveals some similarity, but one striking difference. In equation 5, C_a is dependent upon $P^{3/4}$; in equation 4, upon $P^{4/3}$. Fontenot (4) shows that a dimensional analysis will yield an exponent for P of 3/4 and an equation quite similar to equation 5.

In the work of Centinkale-Fishenden and Laming, the parameter λ appears in the resulting equations. As it was mentioned previously, the value of the wave length of surface waviness is generally unknown. No way of estimating it is available. Thus, in most practical problems, equations 4 and 5 will be of little use. For determining C_a when λ is unknown, a very simple, semi-empirical approach was proposed by Boeschoten and Van der Held (14).

Using intuitive reasoning and an estimation of size and number density of contact spots, Boeschoten and Van der Held derived an expression for C_t. Their expression for C_a is in reality an approximation of that given by Centinkale and Fishenden. Boeschoten and Van der Held approximate the arc-tangent term in equation 1 with $\pi/2$. This, however, is not the only simplifying assumption. Others must be made to eliminate the dependence upon λ.

As it was before, the total contact conductance was written $C_f + C_a$; where $C_f = k_f/\overline{\delta}$. The values of $\overline{\delta}$, reported in reference 14 for air, hydrogen, and helium are:

$$\overline{\delta}_{air} = 0.36(i_A + i_B); \quad \overline{\delta}_{H_2} = 0.76(i_A + i_B); \quad \overline{\delta}_{H_e} = 0.80\ (i_A + i_B)\ .$$

The average value of $\overline{\delta}$, found to be $0.64(i_A + i_B)$, is in excellent agreement with the values found by Centinkale and Fishenden and Laming. The apparent dependence of $\overline{\delta}$ upon the fluid, reported by Boeschoten and Van der Held, was not found in the other two investigations (12 and 13).

The simplified expression for C_a given by Boeschoten and Van der Held is

$$C_a = 1.06 \frac{k_M}{\bar{a}} \left(\frac{P}{H_o} \right) \tag{6}$$

where $\bar{a}$ is the average radius of the contact spots. An approximate value for $\bar{a}$ determined by Boeschoten and Van der Held is 1.2×10^{-3} inches. They report that the value of $\bar{a}$ does not depend upon the materials of which the contacts are made or the contact pressure. This is in agreement with Holm (15). If this average value of $\bar{a}$ is inserted into equation 6, C_a can be expressed simply as

$$C_a = 8.8 \times 10^{-4} \, k_M \frac{P}{H_o} \, . \tag{7}$$

Since all the terms in this equation are known quantities, an approximation for C_a may be obtained. Equation 7 can then be combined with the previous expression for C_f to give the equation for C_t as developed by Boeschoten and Van der Held

$$C_t = \frac{k_f}{\bar{\delta}} + 8.8 \times 10^{-4} \frac{k_M P}{H_o} \tag{8}$$

where $\bar{\delta}$ depends upon the interstitial fluid.

An expression for C_a, somewhat different from those given above, was employed in this study. As explained in detail in reference 4, C_a can be written as

$$C_a = 2 \, n \, \bar{a} \, k_M \tag{9}$$

where n is the number of contact spots per unit area and $\bar{a}$ is the average radius of those spots.

If the various values of $\bar{\delta}$, as found in references 12, 13 and 14 are averaged, $\bar{\delta}$ can be written as

$$\bar{\delta} = 0.64(i_A + i_B) \tag{10}$$

Employing these expressions for C_a and $\bar{\delta}$, C_t can be written as

$$C_t = C_f + C_a = \frac{1.56\ k_f}{(i_A + i_B)} + 2\ n\bar{a}k_M\ . \tag{11}$$

In order to employ this equation i_A, i_B, and $n\bar{a}$ must be determined in terms of known parameters. In reference 4 curves were developed for $n\bar{a}$ as a function of contact pressure. These curves are based on data taken from references 11-14 and are reproduced in Figure 2. Also given in reference 4 is a curve for i/ρ as a function of ρ. This curve is reproduced as Figure 3.

Equation 11 combined with Figures 2 and 3 allows one to obtain, very simply, an estimate of C_t when the R.M.S. value of surface roughness and k_M are known. This estimate should prove useful whenever experimental data are not available. To employ this method one must know the parameters ρ_A, ρ_B, k_M, k_f, P, and T_f--all of which are generally known.

In lieu of equation 11 or one of the more complex expressions, one can go to the literature and attempt to use experimental data. This can be done in many cases, but the end results are not often satisfactory because of the wide divergence of experimental results. This divergence is most apparent in the experimental data compiled by Minges (3) and Fontenot (4).

Thermal Conductance in the Separated Zone

In references 4 and 7 it is shown that the conductance in the separated zone (interface gap) can be divided into three components; i.e. conduction, convection and radiation. It is shown that, in most cases,

convection is not possible and radiation may be neglected. If radiation must be considered, then the gap conductance can be written as

$$C_g = C_R + C_D = k_f \left[\frac{1}{\delta_R} + \frac{1}{\bar{\delta}}\right] \tag{12}$$

where δ_R is given as

$$\delta_R = \frac{k_f}{4\sigma T_M^3} \cdot \tag{13}$$

In the finite difference heat transfer analyses (to be discussed in the following paragraphs) of the two joints for which experimental data were obtained, four situations were considered. These four involved both the aluminum and stainless steel joints at ambient pressure and in vacuum. For the ambient pressure cases $\delta_R \simeq 1900\ \bar{\delta}$ for the aluminum joint and 2000 $\bar{\delta}$ for the stainless steel joint. Thus, there was no question that the heat transfer by radiation across the interface gap could be neglected. For the vacuum cases $\delta_R \simeq 70\ \bar{\delta}$ for the aluminum joint and 30 $\bar{\delta}$ for the stainless steel joint. Here again it was possible to neglect interfacial heat transfer by radiation, without introducing an error in the value of C_g greater than about three percent.

Experimental Temperature Distributions

A series of heat transfer experiments were conducted under controlled conditions to measure the temperature distribution in two bolted joints for a verification of the applicability of equations 11 and 12, and an indirect check of the analytical methods described in reference 10. Two lap joints, one of 6061T6 aluminum and one of 304 stainless steel, were tested.

The aluminum joint consisted of two 7-inch by 2-inch by 1/4-inch plates; the stainless steel plates were the same length and width, but were only 1/8 inch thick. Each plate had seventeen 0.062-inch diameter holes drilled approximately 1/8 inch deep for connecting Conax 32 gauge copper-constantan grounded thermocouples. Figure 4 is a section of the thermocouples. The assembled aluminum joint, along with the hotside circular heating element (Chromalox, Inc.), is shown in Figure 5. Cooling water was fed through the coolant plate with the polyethylene tubing that is visible in Figure 5.

The whole apparatus, with the aluminum joint in place for temperature measurements, is shown in Figures 6 and 7. The aluminum bell jar used for measurements at ambient pressure, as well as in vacuum, is visible in Figure 6.

In Figure 7, a close-up view of the aluminum joint shows the method of thermocouple installation. This attachment method for these thermocouples did not introduce any significant error because of the ceramic insulation sheath around the thermocouple wires (Figure 4). The holes in the plates were drilled to provide an interference fit for the thermocouple tips.

The flow of the cooling water was regulated by a manually operated valve. The inlet and outlet water temperatures were measured at two brass couplings (insulated during tests) in the polyethylene lines (Figure 7). The electrical heating element was controlled by a variac with monitoring of the voltage and current. The output from the 36 thermocouples was registered by two Minneapolis-Honeywell recorders. For tests in a vacuum, the bell jar was evacuated to a pressure between 100 and 300 microns of mercury.

The joint was allowed to come to thermal equilibrium before the desired steady-state temperatures were recorded. This equilibrium was considered attained when temperature measurements were repeatable within $\pm$ 0.5°F for at least 30 minutes.

Ten tests were conducted; nine of these provided a complete set of temperature data. Table 1 summarizes the more important measurements, other than temperature, obtained during these tests.

The steady-state temperature measurements obtained in the nine tests will not be discussed as yet. These measurements will be compared later with temperatures computed in a finite-difference analysis. First, it is necessary to describe the finite-difference steady-state heat transfer technique used to obtain the computed values of joint temperatures.

Calculated Temperatures

The three-dimensional steady-state finite-difference digital program described in reference 9 was used to calculate theoretical values of interface temperature for comparison with the experimental results. As required by the finite-difference method, the two joints were divided into a nodal network, half of which is shown in Figure 8. The locations of the 34 thermocouples are designated by the "O" around the node center point to indicate where measured values of the temperature were available.

Nodes 1-37 (plate 1) were treated as variable-temperature nodes (diffusion nodes); nodes 38-65 (plate 2) were treated as fixed-temperature nodes (boundary nodes). Conductors 23-50 were interface conductors. For handling the convective heat transfer losses and the heat input from the heating element, nodes 1-37 were treated as source nodes.

The thermal conductivity (k) and emittance (ϵ) of the joint materials and the convective heat transfer coefficient (h) were also needed to accurately describe the total heat transfer losses and the heat input from the heating element, nodes 1-37 were treated as source nodes.

The thermal conductivity (k) and emittance (ϵ) of the joint materials and the convective heat transfer coefficient (h) were also needed to accurately describe the total heat transfer problem. Because the values given in the literature would only be estimates in this case, 10 thermocouples, located in the two plates outside of the lap area, provided temperature measurements not directly influenced by the interface conductance. From these data, the constants, k, ϵ, and h were determined for the aluminum and stainless steel joints. A summary of the computed values is given in Table 2 along with estimated values taken from the literature. In most cases the computed value was used in the finite-difference analysis; however, in some cases the value obtained from the literature was used. A detailed discussion of the determination of k, ϵ, and h is given in reference 7.

The actual division of the joint heat losses into convection and radiation losses, was found to be unimportant in the finite-difference steady-state analysis--as long as the total heat loss was accounted for. In addition, if the total heat loss rate is small compared with the heat transfer rate across the joint, no appreciable error is introduced into the computed interface temperature differences. The computed heat transfer rates to and from the joints for all 10 tests are given in Table 3.

To obtain the rates of heat input (q_1) given in Table 3, the measures values of the heating element input were corrected for convection

and radiation losses about the heating element by use of the calculated values of h and ϵ. The heat transfer loss for all 34 thermocouples inserted in the plates was found to be only 0.008 Btu/min.

With k, ϵ, h and q_1 determined, the only remaining parameters to be determined for use in the finite-difference analyses were the interface thermal conductances (conductors 23-50). The values of the thermal conductance between pairs of interface nodes were obtained using equation 11 to calculate C_t in the contact area and equation 12 to calculate C_g in the gap area. The results for these representative tests (1, 5 and 8) are given in Tables 4, 5 and 6. The values of k_f for these equations were taken from reference 4 and the values of i_A and i_B (irregularity of the plate surfaces) were measured with a Proficorder (Micrometrical Corporation). The average measured values for the stainless steel and aluminum plates are plotted in Figure 3 and are seen to fall within the standard deviation of the data from reference 4.

The contact areas for the stainless steel and aluminum joints were determined from reference 10. The experimental data reported in that reference for the one-inch button-head bolt was extrapolated to the 3/8-inch button-head bolt actually used in the joints. To obtain values of the radial extent of the interface stress from Figure 18 of reference 10, a value of 0.336 inch was used for r_h rather than the actual bolthead radius of 0.406 inch, in line with the oil pressure and penetration data given for button-head bolts in that same paper.

Average values of the interface gap thickness, $\bar{\delta}$, were determined from joint plate deflections calculated using the analysis described in reference 10. The results for tests 1, 5, and 8 are given in Tables 4, 5 and 6.

The contact-area interface pressures were determined with Fernlund's simplified method discussed in references 7 and 10. These pressures for tests 1, 5 and 8 are also given in Tables 4, 5 and 6. This method was suitable for the joints under consideration because the values of $(r_\sigma - r_s)$ are close to the values of $(r_h - r_s)$. The calculated interface stress distributions (those for the 15 ft-lbs torque are shown in Figure 9) were used to find values of $\overline{na}$ from the curve labeled "arithmetic mean" in Figure 2.

In Tables 4, 5 and 6, besides the values of C_g, C_t, $\overline{\delta}$, and average contact pressure, the values of $\overline{na}$ read for each of the interface conductors from Figure 2 are given. Also given in these tables are the percentages of the interface nodal area in which gap conductance (C_g) occurs and in which contact conductance (C_t) occurs.

From the tables, it is apparent that the conductance between most of the interfacial nodal pairs is governed by the equation for C_g. This is especially pronounced in the stainless steel joint (tests 5 and 8). The differences in the average values of the interface gap $\overline{\delta}$ are also apparent from the three tables. The difference in the values of $\overline{\delta}$ for tests 5 and 8 is due to the difference in the applied torque (see Table 1). A comparison of the values of C_g and nodal interface conductance for tests 5 and 8 reveals the effect of interface fluid pressure on the magnitude of the interface conductance.

The values of the nodal interface conductances resulting from the complete analyses for the nine tests are shown in Table 7. These values were used in the finite-difference analyses to determine the interface temperature distributions. The computed values of interface temperatures are discussed in the following paragraphs.

Comparison Between Theoretical and Measured Values of Interface Temperatures

Steady-state temperature distributions were calculated with the finite-difference computed program (reference 9) and the nodal arrangement shown in Figure 8. The temperature distributions were found for each of the nine tests using the data in Tables 2, 3 and 7.

In Table 8, the computed temperatures for test 1 are tabulated for comparison with the measured temperatures, which are also tabulated. Similar tables for tests 2-10 are given in reference 7. A summary of the differences between theoretical and experimental temperature gradients for all of the tests is given in Table 9.

From Table 8 it is apparent that the average percentage deviation between theoretical and experimental values of ΔT is large in most cases. The over-all average deviation for the nine tests was 35 percent. However, it is clear from Table 9 that the average values of the absolute deviation are on the order of $2^{\circ}F$. This is within the limits of the accuracy of the temperature measurements and the finite-difference analysis, the latter being limited by the knowledge of k, h and ϵ.

Summary and Conclusions

A practical analytical method was developed to predict the interface thermal conductance of a bolted joint from a minimum of design information. Simple equations were developed to describe the thermal conductance across the interfacial contact zone and the interface gap. Use was made of methods, described in a previous paper (10), to determine the interfacial contact pressures and the width of the interface gap. Calculated

values of interface conductances were used in finite-difference heat transfer analyses and the computed interface temperatures compared to values measured in nine experiments.

Measured values of the temperature drop across the joint interfaces ranged from 0.3 to 17.5°F, while the calculated values ranged from 0.1 to 23.2°F. The average difference between measured and calculated interfacial temperature drops was 35 percent or 2°F.

In reviewing the literature, large discrepancies were found between and within sets of experimental data for interface thermal conductance. Agreement to within 35 percent was rarely found. Difficulties inherent in the experimental measurements are part of the reason. In light of this, the analytical method developed in this study provides a better method of obtaining estimates of interface thermal conductance values for design purposes.

Acknowledgements

The authors wish to thank the National Science Foundation and The National Aeronautics and Space Administration for their financial support. This study was substantially supported by funds provided under NASA Grant NGR- Number 19-001-35.

Bibliography

1. "Some Aspects of Heat Flow," E. F. Northrup, Transactions of American Electrochemical Society, XXIV, 1913, pp. 85-103.

2. Bibliography on Thermal Metallic Contact Conductance, H. L. Atkins, NASA TM X-53227, April 15, 1965.

Bibliography (continued)

3. "Thermal Contact Resistance - A Review of the Literature," M. L. Minges, Air Force Materials Laboratory, AFML-TR-65-375-Volume I, Wright-Patterson A.F.B., Ohio, April 1966.

4. "Thermal Conductance of Contacts and Joints," J. E. Fontenot, Jr., Boeing Document D5-12206, The Boeing Company, Huntsville, Alabama, December 1964.

5. "Heat Transfer of Proposed Structural Joints in the Rocket Package for the F-86D Airplane," J. Jelinek, North American Aviation Lab Report No. NA-49-831, September 30, 1949.

6. "Studies in Heat Transfer in Aircraft Structure Joints," K. G. Lindh et al, UCLA Report 57-50, University of California in Los Angeles, May 1957.

7. "The Thermal Conductance of Bolted Joints," J. E. Fontenot, Jr., Ph.D. Dissertation, Louisiana State University, Baton Rouge, Louisiana, January 1968.

8. "Boeing Thermal Analyzer," no author, Boeing Document AS0313, The Boeing Company, Seattle, Washington, August 1963.

9. "Chrysler Improved Numerical Differencing Analyzer," J. D. Gaski and D. R. Lewis, Chrysler Corporation Space Division TN-AP-66-15, New Orleans, Louisiana, April 1966.

10. "Prediction of Interfacial Stress and Gap in a Bolted Joint," J. E. Fontenot, Jr. and C. A. Whitehurst, Paper Submitted for Presentation at the Annual Aviation and Space Division Conference, June 16-19, 1968.

11. "Prediction of Thermal Conductance of Metallic Surfaces in Contact," H. Fenech and W. H. Rohsenow, Journal of Heat Transfer, 85:1, February 1963, pp. 15-24.

12. "Thermal Conductance of Metal Surfaces in Contact," T. N. Centinkale and M. Fishenden, General Discussion on Heat Transfer, IME and ASME, 1951, pp. 271-294.

13. "Thermal Conductance of Machined Contacts," L. C. Laming, International Developments in Heat Transfer, The American Society of Mechanical Engineers, New York, 1963, pp. 65-76.

14. "The Thermal Conductance of Contacts Between Aluminum and Other Metals," F. Boeschoten and E. F. M. Van der Held, Physica, XXIII, 1957, pp. 37-44.

15. Electrical Contacts, R. Holm, Almquist and Wiksells Akademiska Hanbocker, Stockholm, Sweden, 1946.

16. Heat Transmission, W. H. McAdams, McGraw-Hill Book Company, Inc., New York, N.Y., 1954, p. 6.

17. "Materials Selector Issue," Materials in Design Engineering, 54:5, October 1961.

18. "Thermophysical Properties of Materials," G. Belleman, The Boeing Company, Document No. D-16103-1, Seattle, Washington, March 1961.

Table 1

SUMMARY OF HEAT TRANSFER TESTS

Test No.	Joint	Torque ft-lbs	Ambient Press. ~ psi	Heater Current ~ amps	Heater Voltage ~ volts	Flow Rate of Water ~ lb_m/min
1	Alum.	15	14.7	0.92	95.	2.34
2	"	8	14.7	0.92	95.	"
3	"	8	0.0058	0.85	86.5	"
4	"	15	0.0039	0.85	86.5	"
5	Stainless Steel	8	14.7	0.625	66.	"
6	"	8	0.0019	0.38	40.	"
7	"	15	14.7	0.64	66.	"
8	"	15	0.0025	0.38	40.5	"
10	"	15	14.7*	0.65	68.	"

*Bell jar not used.

Table 2

THERMAL CONDUCTIVITY, EMITTANCE, AND CONVECTIVE FILM COEFFICIENTS

		k BTU/in-min-^oF	ϵ	h BTU/min-in^2-^oF
6061 Aluminum	Reference 16		0.10-0.15	
	" 17	0.154		
	Reference 18	0.138	0.56 (anodized)	
	Joint Data	0.160	0.59	0.80×10^{-4}
	Value Used	0.160	0.15	1.74×10^{-4}
304 Stainless	Reference 16		0.30	
	" 17	0.0133		
	" 18	0.0130-0.0135	0.30-0.41	
	Joint Data	0.0147	0.34	2.55×10^{-4}
	Value Used	0.0147	0.34	2.55×10^{-4}
	Reference 16			1.74×10^{-4}

Table 3

CALCULATED JOINT HEAT TRANSFER AND LOSS RATES

Test	Input Heat Rate BTU/min	Output Heat Rate BTU/min	Heat Loss Rate Across Joint BTU/min
1	4.20	3.53	0.67
2	4.20	3.53	0.67
3	3.74	3.33 (3.64)*	0.41 (0.10)*
4	3.74	3.33 (3.64)*	0.41 (0.10)*
5	0.58	0.13	0.45
6	0.32	0.17	0.15
7	0.64	0.14	0.50
8	0.33	0.18	0.15
9	0.32	0.16	0.16
10	0.75	0.12	0.63

*Value used in finite-difference analysis.

Table 4

INTERMEDIATE RESULTS IN THE CALCULATION OF THE NODAL INTERFACE CONDUCTANCES - TEST 1

Conductor Number	$\overline{\delta}$	C_g	Avg Contact Pressure	$\overline{na}$	C_t	Percent C_g	Percent C_t	Nodal Interf. Conductance
	10^{-4} in	$\frac{BTU}{min\ in^2\ °F}$	psi	1/in	$\frac{BTU}{min\ in^2\ °F}$			$\frac{BTU}{min\ in^2\ °F}$
23	6.0	0.041	90.	0.29	0.17	90.	10.	0.055
24	3.9	0.063	650.	1.6	0.59	50.	50.	0.33
25	4.7	0.052	30.	0.12	0.12	75.	25.	0.068
26	5.2	0.047	-	-	-	100.	0.	0.047
27	7.0	0.035	-	-	-	100.	0.	0.035
28	5.2	0.047	-	-	-	100.	0.	0.047
29	4.7	0.052	30.	0.12	0.12	75.	25.	0.068
30	3.9	0.063	650.	1.6	0.59	50.	50.	0.33
31	6.0	0.041	90.	0.29	0.17	90.	10.	0.055
32	4.5	0.054	650.	1.6	0.59	50.	50.	0.33
33	-	-	2700.	5.8	1.9	0.	100.	1.9
34	-	-	800.	2.0	0.72	0.	100.	0.72
35	3.2	0.076	90.	0.29	0.17	50.	50.	0.12
36	3.7	0.066	-	-	-	100.	0.	0.067
37	3.2	0.076	90.	0.29	0.17	50.	50.	0.12
38	-	-	800.	2.0	0.72	0.	100.	0.72
39	-	-	2700.	5.8	1.9	0.	100.	1.9
40	4.5	0.054	650.	1.6	0.59	50.	50.	0.33
41	6.0	0.040	90.	0.29	0.17	90.	10.	0.053
42	3.9	0.061	650.	1.6	0.59	50.	50.	0.33
43	4.7	0.051	30.	0.12	0.12	75.	25.	0.068
44	5.2	0.046	-	-	-	100.	0.	0.046
45	7.0	0.034	-	-	-	100.	0.	0.034
46	5.2	0.046	-	-	-	100.	0.	0.046
47	4.7	0.051	30.	0.12	0.12	75.	25.	0.066
48	3.9	0.061	650.	1.6	0.59	50.	50.	0.33
49	6.0	0.040	90.	0.29	0.17	90.	10.	0.053
50	3.8	0.064	-	-	-	100.	0.	0.062

Table 5

INTERMEDIATE RESULTS IN THE CALCULATION OF THE NODAL INTERFACE CONDUCTANCES - TEST 5

Conductor Number	$\bar{\delta}$	C_g	Avg Contact Pressure	$\bar{na}$	C_t	Percent C_g	Percent C_t	Nodal Interf. Conductance
	10^{-4} in	$\frac{BTU}{min\ in^2\ °F}$	psi	1/in	$\frac{BTU}{min\ in^2\ °F}$			$\frac{BTU}{min\ in^2\ °F}$
23	2.7	0.085	-	-	-	100.	0.	0.086
24	1.7	0.14	150.	0.45	0.15	90.	10.	0.14
25	2.1	0.11	-	-	-	100.	0.	0.11
26	2.5	0.092	-	-	-	100.	0.	0.092
27	2.6	0.089	-	-	-	100.	0.	0.088
28	2.5	0.092	-	-	-	100.	0.	0.092
29	2.1	0.11	-	-	-	100.	0.	0.11
30	1.7	0.14	150.	0.45	0.15	90.	10.	0.14
31	2.7	0.085	-	-	-	100.	0.	0.086
32	2.0	0.11	150.	0.45	0.14	90.	10.	0.12
33	0.45	0.51	2200.	4.8	0.27	5.	95.	0.28
34	1.1	0.21	150.	0.45	0.14	80.	20.	0.19
35	1.3	0.18	-	-	-	100.	0.	0.17
36	1.6	0.14	-	-	-	100.	0.	0.14
37	1.3	0.18	-	-	-	100.	0.	0.17
38	1.1	0.21	150.	0.45	0.14	80.	20.	0.19
39	0.45	0.51	2200.	4.8	0.27	5.	95.	0.28
40	2.0	0.11	150.	0.45	0.14	90.	10.	0.12
41	2.7	0.083	-	-	-	100.	0.	0.86
42	1.7	0.13	150.	0.45	0.14	90.	10.	0.13
43	2.1	0.11	-	-	-	100.	0.	0.11
44	2.5	0.090	-	-	-	100.	0.	0.092
45	2.6	0.087	-	-	-	100.	0.	0.086
46	2.5	0.090	-	-	-	100.	0.	0.092
47	2.1	0.11	-	-	-	100.	0.	0.11
48	1.7	0.13	150.	0.45	0.14	90.	10.	0.13
49	2.7	0.083	-	-	-	100.	0.	0.86
50	1.7	0.13	-	-	-	100.	0.	0.13

Table 6

INTERMEDIATE RESULTS IN THE CALCULATION OF THE NODAL INTERFACE CONDUCTANCES - TEST 8

Conductor Number	$\bar{\delta}$	C_g	Avg Contact Pressure	$\bar{n}\bar{a}$	C_t	Percent C_g	Percent C_t	Nodal Interf. Conductance
	10^{-4} in	$\frac{BTU}{min\ in^2\ °F}$	psi	1/in	$\frac{BTU}{min\ in^2\ °F}$			$\frac{BTU}{min\ in^2\ °F}$
23	5.4	0.0012	-	-	-	100.	0.	0.0012
24	3.6	0.0012	200.	0.59	0.019	90.	10.	0.0012
25	4.3	0.0011	-	-	-	100.	0.	0.0011
26	4.8	0.0011	-	-	-	100.	0.	0.0011
27	5.5	0.0012	-	-	-	100.	0.	0.0012
28	4.8	0.0011	-	-	-	100.	0.	0.0011
29	4.3	0.0011	-	-	-	100.	0.	0.0011
30	3.6	0.0012	200.	0.59	0.019	90.	10.	0.0012
31	5.4	0.0012	-	-	-	100.	0.	0.0012
32	4.1	0.0012	200.	0.59	0.019	90.	10.	0.0012
33	0.9	0.00078	4500.	9.0	0.26	5.	95.	0.25
34	2.2	0.0011	200.	0.59	0.019	80.	20.	0.0046
35	3.1	0.0011	-	-	-	100.	0.	0.0011
36	3.4	0.0012	-	-	-	100.	0.	0.0012
37	3.1	0.0011	-	-	-	100.	0.	0.0011
38	2.2	0.0011	200.	0.59	0.019	80.	20.	0.0046
39	0.9	0.00078	4500.	9.0	0.26	5.	95.	0.25
40	4.1	0.0012	200.	0.59	0.019	90.	10.	0.0012
41	5.4	0.0012	-	-	-	100.	0.	0.0012
42	3.6	0.0012	200.	0.59	0.019	90.	10.	0.0012
43	4.3	0.0011	-	-	-	100.	0.	0.0011
44	4.8	0.0011	-	-	-	100.	0.	0.0011
45	5.5	0.0012	-	-	-	100.	0.	0.0012
46	4.8	0.0011	-	-	-	100.	0.	0.0011
47	4.3	0.0011	-	-	-	100.	0.	0.0011
48	3.6	0.0012	200.	0.59	0.019	90.	10.	0.0012
49	5.4	0.0012	-	-	-	100.	0.	0.0012
50	3.4	0.0012	-	-	-	100.	0.	0.0012

Table 7

THEORETICAL VALUES OF INTERFACE CONDUCTANCE

Conductor No.	Interface Conductance BTU/in^2 - min ^oF								
	Test 1	Test 2	Test 3	Test 4	Test 5	Test 6	Test 7	Test 8	Test 10
23	.055	.092	.0081	.011	.086	.00088	.042	.0012	.042
24	.33	.25	.15	.27	.14	.0025	.073	.0012	.073
25	.068	.092	.057	.012	.11	.00083	.054	.0011	.052
26	.047	.10	.0028	.0018	.092	.00091	.049	.0011	.048
27	.035	.083	.0029	.0019	.088	.00091	.042	.0012	.041
28	.047	.10	.0028	.00018	.092	.00091	.049	.0011	.048
29	.068	.092	.057	.012	.11	.00083	.054	.0011	.052
30	.33	.25	.15	.26	.14	.0025	.073	.0012	.073
31	.055	.092	.0081	.011	.086	.00088	.042	.0012	.042
32	.33	.22	.15	.26	.12	.0023	.064	.0012	.064
33	1.9	1.0	.96	1.86	.28	.13	.39	.25	.39
34	.72	.42	.34	.64	.19	.022	.11	.0046	.11
35	.12	.14	.028	.26	.17	.00093	.075	.0011	.075
36	.067	.13	.0027	.0018	.14	.00093	.067	.0012	.067
37	.12	.14	.028	.049	.17	.00093	.075	.0011	.075
38	.72	.42	.34	.71	.19	.022	.11	.0046	.11
39	1.9	1.0	.96	1.86	.28	.13	.39	.25	.39
40	.33	.22	.15	.26	.12	.0023	.064	.0012	.064
41	.053	.092	.0081	.011	.86	.00088	.042	.0012	.042
42	.33	.25	.15	.26	.13	.0025	.073	.0012	.073
43	.068	.092	.057	.012	.11	.00083	.053	.0011	.051
44	.046	.10	.0028	.0018	.092	.00091	.047	.0011	.046
45	.034	.086	.0029	.0022	.086	.00090	.041	.0012	.040
46	.046	.10	.0028	.0018	.092	.00091	.047	.0011	.046
47	.066	.092	.057	.012	.11	.00083	.053	.0011	.052
48	.33	.25	.15	.26	.13	.0025	.073	.0012	.073
49	.053	.092	.0081	.011	.86	.00088	.042	.0012	.042
50	.062	.14	.0025	.020	.13	.0010	.068	.0012	.065

Table 8

INTERFACE TEMPERATURES FOR TEST 1

CONDUCTOR NO.	COLD SIDE TEMP. ~ °F	HOT SIDE TEMP. ~ °F		Δ T ACROSS INTERFACE ~ °F		% DEVIATION IN Δ T
		MEASURED	CALCULATED	MEASURED	CALCULATED	
24	178.4	185.2	182.9	6.8	4.5	-34.
27	174.8	185.1	184.4	10.3	9.6	- 6.8
30	176.2	183.5	180.8	7.3	4.6	-37.
32	173.5	175.7	174.6	2.2	1.1	-50.
35	173.3	174.2	174.6	0.9	1.3	44.
36	171.7	174.4	174.0	2.7	2.3	-15.
41	159.6	167.7	167.8	8.1	8.2	- 1.2
42	162.2	167.1	165.8	4.9	3.6	-26.
43	160.6	166.3	167.3	5.7	6.7	18.
45	159.2	168.9	167.6	9.7	8.4	-13.
48	158.9	166.4	163.0	7.5	4.1	-45.
50	165.6	171.6	170.2	6.0	4.6	-23.
		Absolute Average		6.0	4.9	26.

Table 9

COMPARISON OF THEORETICAL AND EXPERIMENTAL INTERFACE TEMPERATURE DROPS

Conductor Number	Deviation in Interface Temperature Drop ~°F								
	Test 1	Test 2	Test 3	Test 4	Test 5	Test 6	Test 7	Test 8	Test 10
24	-2.3	-2.4	-2.2	-4.4	-3.5	2.2	-2.7	5.4	-2.5
27	-0.7	-2.5	-1.6	-3.3	-3.8	3.0	-4.0	5.8	-1.2
30	-2.7	-4.0	-0.2	-5.3	-1.2	5.6	-2.0	6.2	-0.9
32	-1.1	-2.8	-0.7	-0.7	-1.3	0.3	-1.4	4.1	-1.4
35	0.4	-0.6	-1.7	-3.3	-1.5	-0.2	-0.9	2.8	0.9
36	-0.4	-1.6	-1.5	-3.0	-	1.1	-0.4	2.4	-0.2
41	0.1	-1.8	1.4	-0.6	-0.8	2.1	-2.3	3.2	-2.5
42	-1.3	-1.8	-0.9	-4.6	-1.3	-1.3	-0.4	2.0	-1.7
43	1.0	-0.2	0.6	-0.2	-2.2	0.2	-2.9	2.4	-1.5
45	-1.3	-2.7	-1.5	-0.9	-2.0	-0.6	-2.8	1.3	-1.9
48	-3.4	-3.6	-4.8	-6.4	-5.6	-	-	-	-
50	-1.4	-2.5	1.8	-1.8	-3.6	0.1	-3.1	1.6	-0.3
Average Abs. Dev.	1.3	2.2	1.6	2.9	2.4	1.5	2.1	3.4	1.4
Overall Average Deviation = 2.1°F									

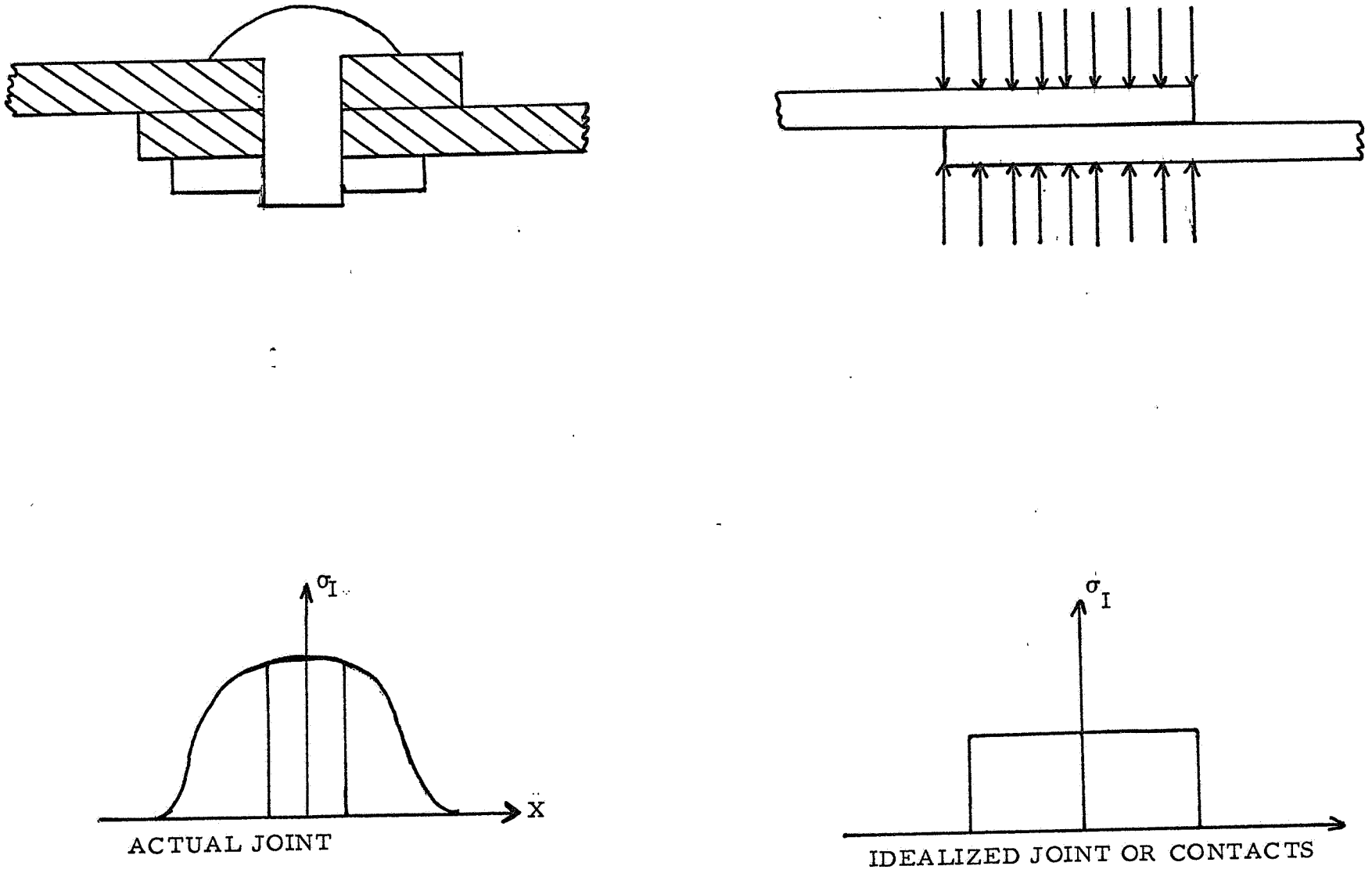

FIGURE 1 ACTUAL JOINT VERSUS IDEALIZED JOINT OR CONTACTS

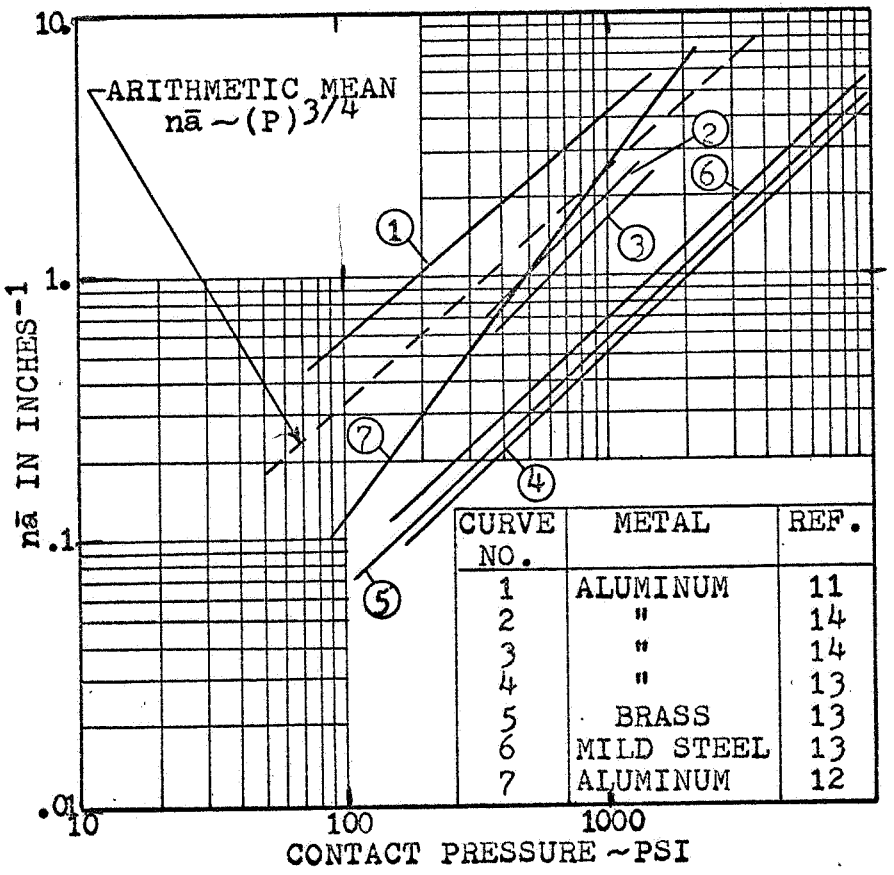

FIGURE 2 $\bar{na}$ Versus Contact Pressure

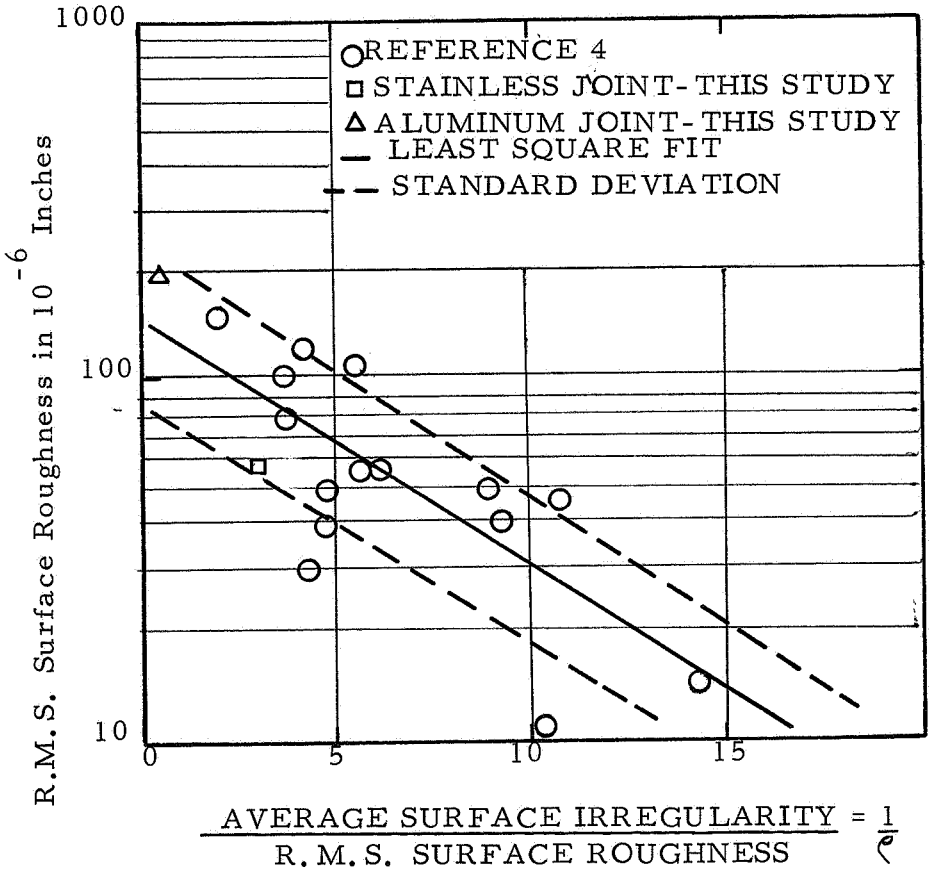

FIGURE 3 The Ratio of Average Surface Irregularity to R.M.S. Surface Roughness Versus R.M.S. Surface Roughness

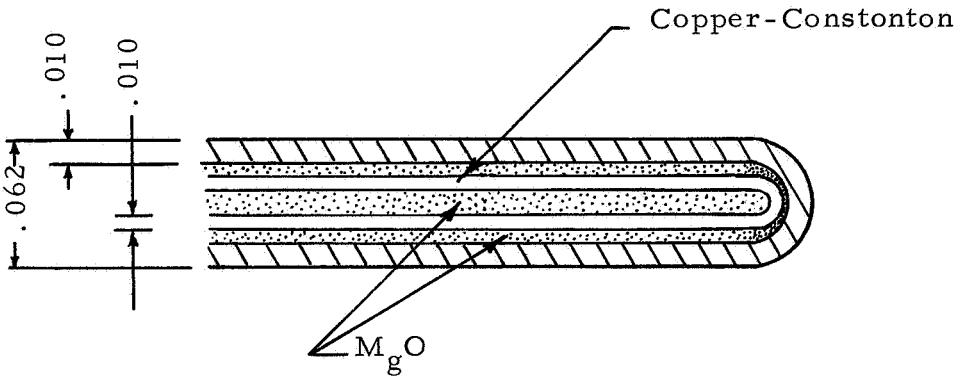

FIGURE 4 Section of Thermocouple

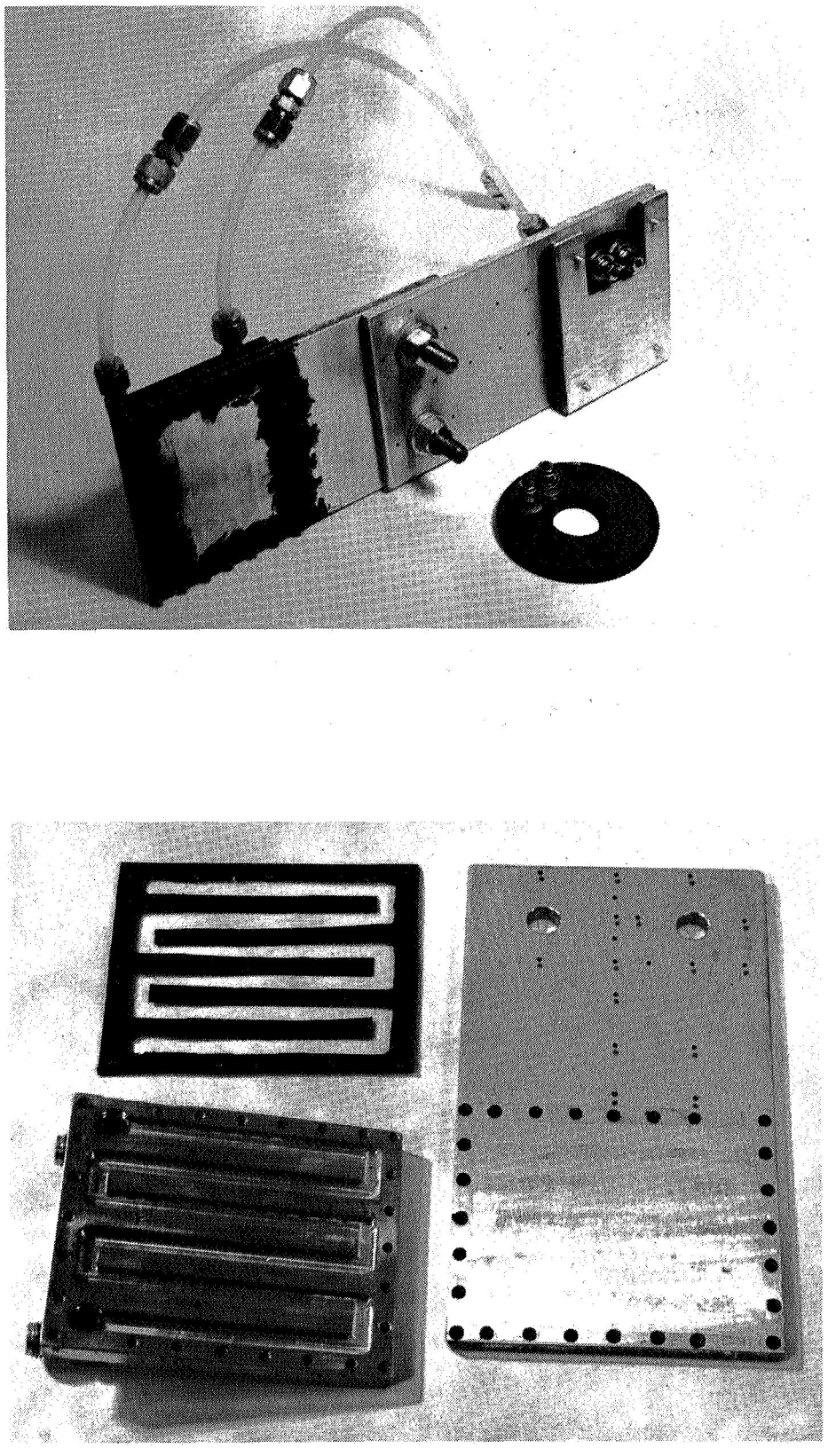

Figure 5 Aluminum Joint Used in Heat Trasfer Study

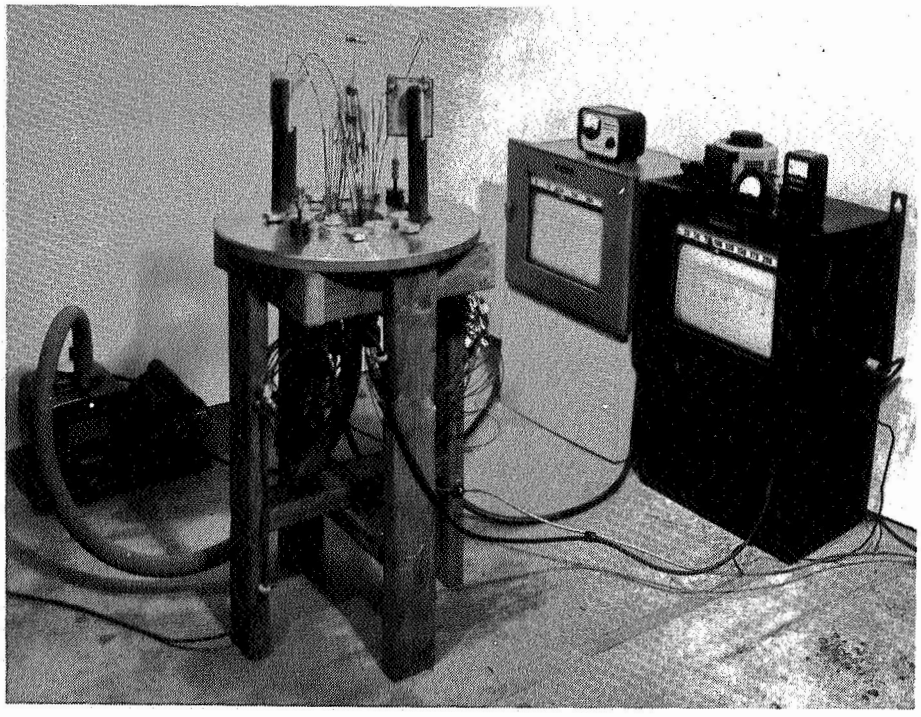

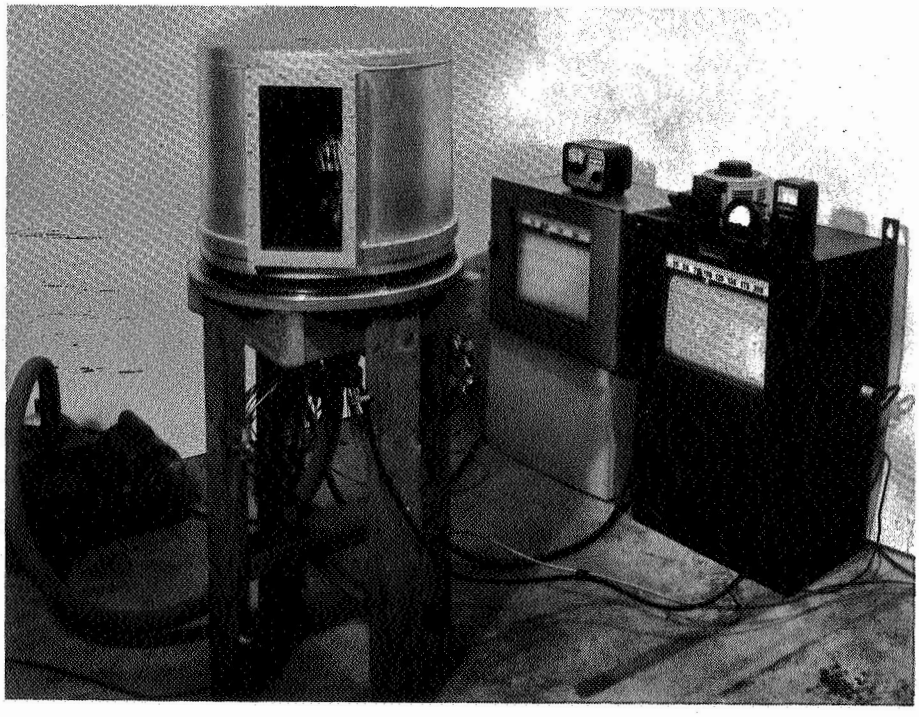

FIGURE 6 EXPERIMENTAL ARRANGEMENT FOR HEAT TRANSFER STUDY (BELL JAR IN PLACE)

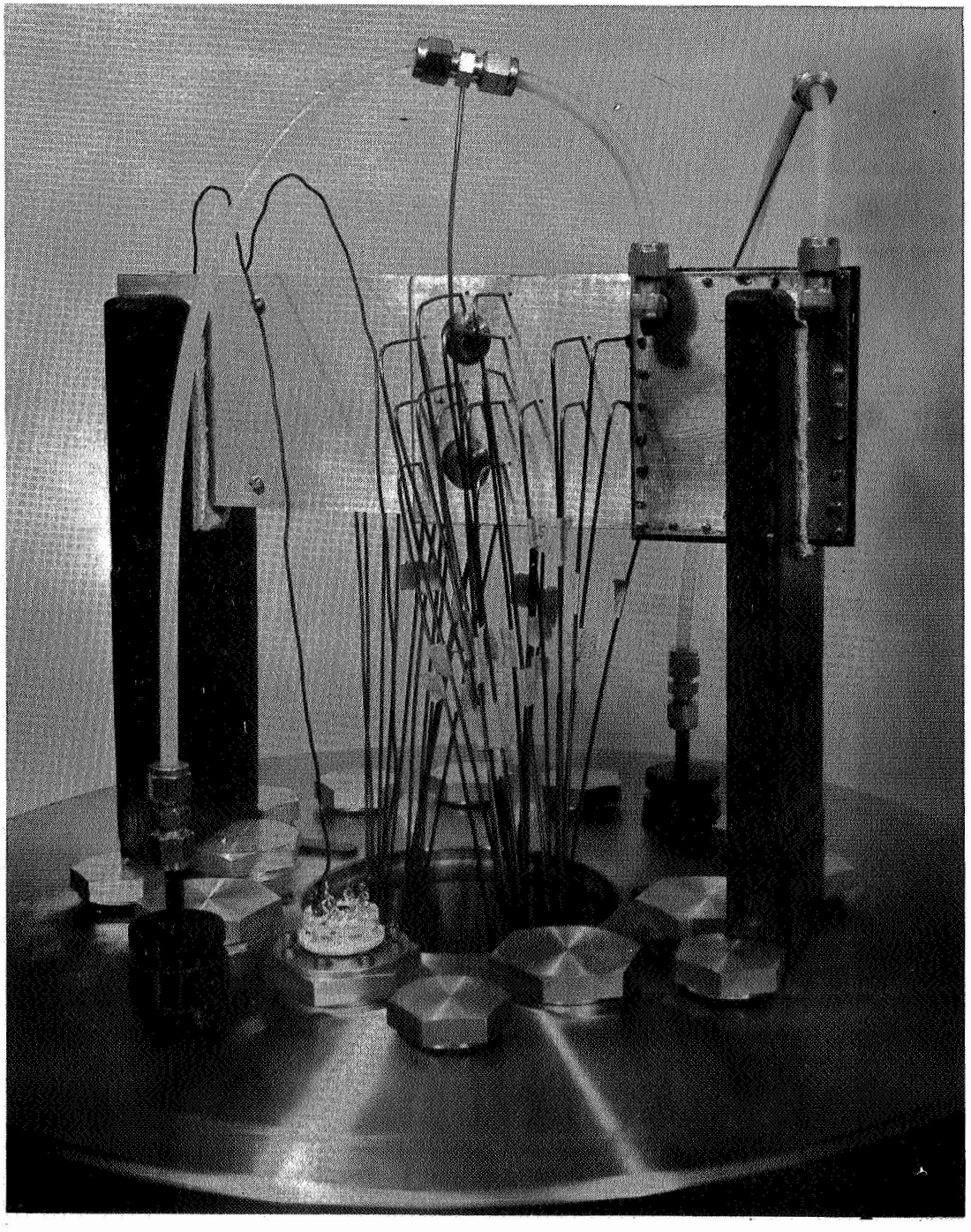

FIGURE 7 CLOSE-UP VIEW – ALUMINUM JOINT INSTALLED FOR HEAT TRANSFER STUDY

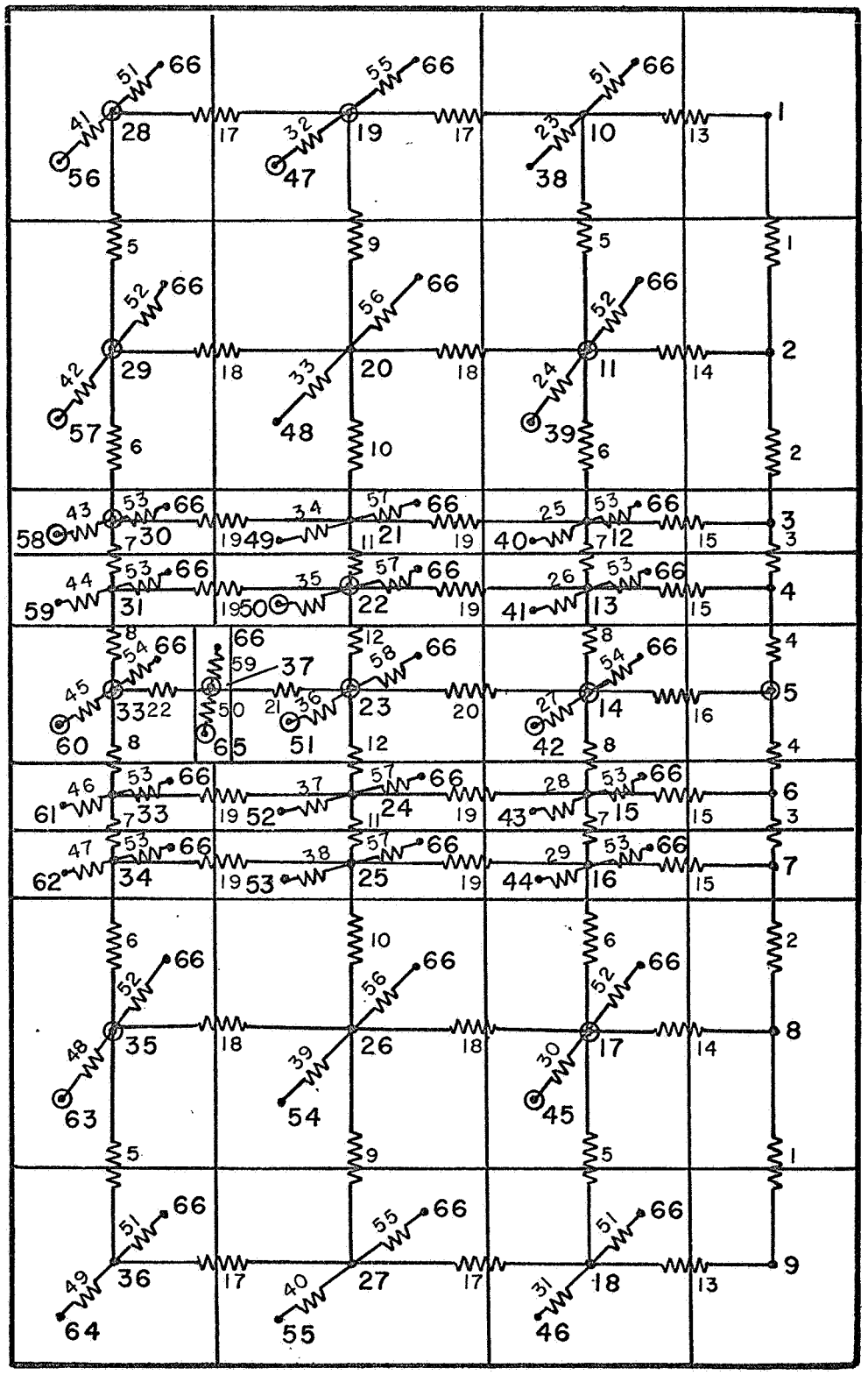

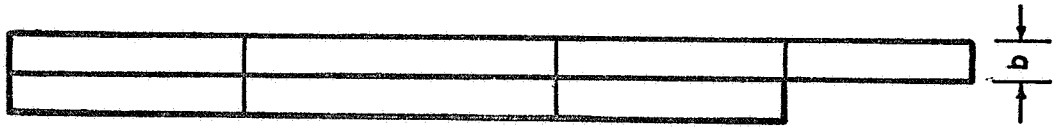

FIGURE 8 NODAL NETWORK FOR FINITE DIFFERENCE ANALYSES

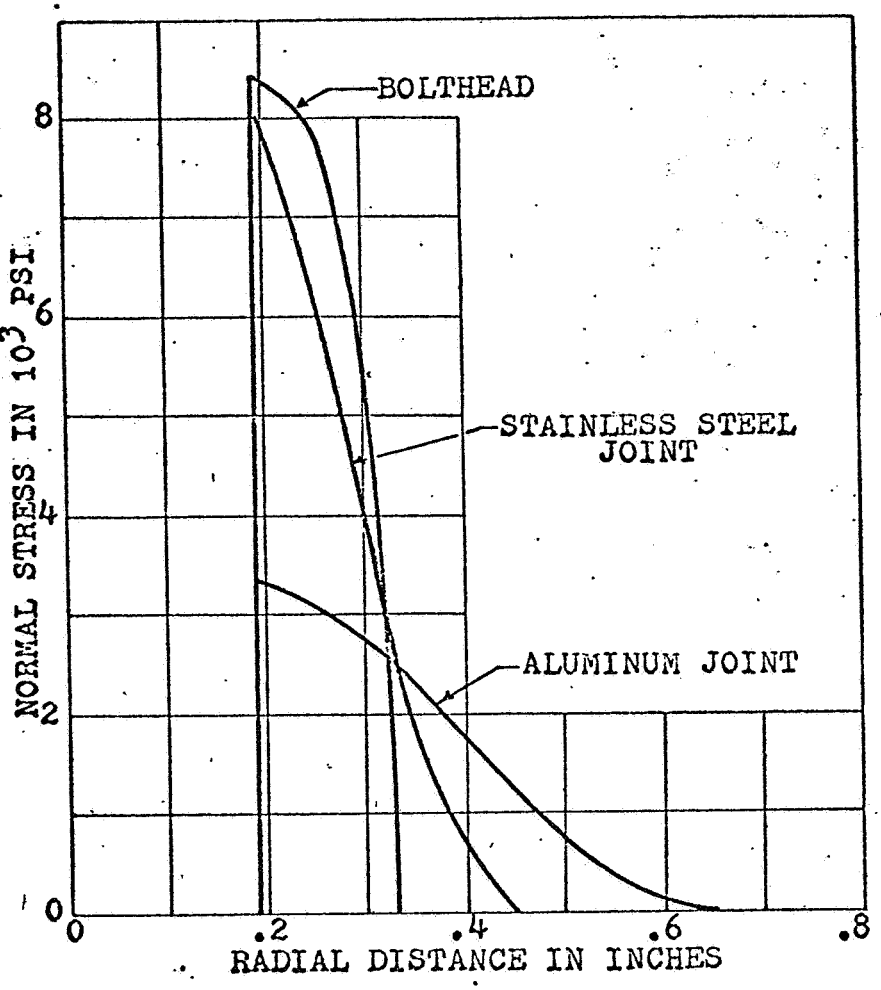

FIGURE 9 Bolthead and Interface Stress Distribution for 15 ft-lbs Torque